Haptic-Enabled Handheld Mobile Robots: Design and Analysis

Ayberk Özgür[1], Wafa Johal[1,2], Francesco Mondada[2], Pierre Dillenbourg[1]
[1]CHILI, [2]LSRO, EPFL
Lausanne, Switzerland
{name.surname}@epfl.ch

ABSTRACT

The Cellulo robots are small tangible robots that are designed to represent virtual interactive point-like objects that reside on a plane within carefully designed learning activities. In the context of these activities, our robots not only display autonomous motion and act as tangible interfaces, but are also usable as haptic devices in order to exploit, for instance, kinesthetic learning. In this article, we present the design and analysis of the haptic interaction module of the Cellulo robots. We first detail our hardware and controller design that is low-cost and versatile. Then, we describe the task-based experimental procedure to evaluate the robot's haptic abilities. We show that our robot is usable in most of the tested tasks and extract perceptive and manipulative guidelines for the design of haptic elements to be integrated in future learning activities. We conclude with limitations of the system and future work.

ACM Classification Keywords

H.5.2. User Interfaces: Haptic I/O; I.2.9. Robotics

Author Keywords

Haptic interaction; Mobile robots; Handheld robots

INTRODUCTION

Within the *Cellulo* project, we are in the process of exploring the novel concept of handheld mobile haptic robots that operate on printed paper sheets (seen in use in Figure 1) and its applicability to education. Our premise is that small-sized graspable mobile robots, if appropriately designed, can be used as an interface for interacting with many virtual point-like objects that reside on a plane. Here, the robots represent the spatial presence and motion of these objects while responding to the user haptically upon physical interaction (*e.g.* conveying virtual forces that act on the objects); in this sense, the robots act as "autonomous mice". Moreover, multiple robots can autonomously come together to form arbitrary shapes and forms, enhancing the representation and interaction capabilities.

We imagine Cellulo as the union of such robots and carefully designed activities where each activity is built to teach a well-defined and well-contained notion. Each activity is housed on a poster-sized printed activity sheet containing necessary graphics; robots that are released on this sheet start working instantly. One powerful aspect of this proposed concept is that it provides physical interaction points (tangible and haptic) within the activity to the learners that are working separately or collaboratively through many robots. These points of interaction may be allocated to singular learners, possibly within groups (as in [29] where learners each have one "hot air balloon" to "feel the winds" on a geographical map to learn the wind formation through atmospheric pressure) or may be shared among the group (as in the chemistry concept presented in [30] where learners freely interact with "particle"s, feeling inter-atomic and inter-molecular forces in a "test chamber" to form and break molecules and play with pressure/temperature). The long term goal of the Cellulo project is to build, using these haptic-enabled tangible robots (among other elements) to create a versatile, ubiquitous, robust and low-cost tool for education that touches vast areas of curricula; [30] includes in-depth discussions about our project's goals and motivations.

Figure 1. The Cellulo robot, conveying an otherwise hidden orientation by means of haptic feedback. By designing and assessing such "atoms" of haptic user interaction, we aim to show the usability of our robot as a haptic device and extract perceptive and manipulative measures for designing haptic elements for our learning activities.

In this article, we focus on the design of the haptics subsystem within the Cellulo robot and its characterization, in order to be able to use haptic information in future learning activities using this design. We propose to tackle this problem by building and evaluating atomic haptic interactions that will be easily integrable in future educational activities. Using this evaluation procedure, we aim to address two research challenges in this paper: (i) Show that our robot is applicable as a haptic device for these "atoms", (ii) Compile reference measures for the use of these "atoms" (guidelines on sensitivity and maximal capacity for planar haptic feedback).

CHI 2017, May 06 - 11, 2017, Denver, CO, USA

ISBN 978-1-4503-4655-9/17/05…$15.00

DOI: http://dx.doi.org/10.1145/3025453.3025994

We first give a brief overview of the previous work found in literature that is related to various aspects of our work. Then, we provide the details of our own design and implementation. Next, we present our methodology, analysis and measures to characterize our proposed platform. Finally, we discuss our findings and give our outlook and future work.

RELATED WORK

The device we present in this paper, namely the Cellulo robot, is a handheld mobile robot that serves as a full 3DOF (x, y, θ) haptic device with practically unlimited workspace (it operates on encoded paper sheets, as large as A0, that can be stitched together indefinitely), and is therefore usable as a desktop tangible item. It is built upon and inspired from works found in numerous fields such as haptic device design and control, mobile haptic interfaces and active tangible interfaces.

2DOF (x, y) or 3DOF (x, y, θ) planar haptic devices, comparable to ours, can be used as interfaces to point-like objects residing on a plane. [1] gives one of the first examples in the literature of what can be called a "haptic mouse". It operates on a conductive surface and can resist the user's motion by means of the force generated by controlled eddy currents (same method as described in [15]) for *kinesthetic feedback* and can pulse the left mouse button for *tactile feedback*. While being relatively more complex and higher-cost, our design is conceived to not only apply forces in opposite direction of the current motion of the device but in any direction at any time.

The literature on mice with practically unlimited workspace (such as [1] and our design) was mainly reserved to tactile feedback (found mainly in patents and numerous commercial products released in the past two decades) while the focus on kinesthetic feedback remained exclusive to grounded desktop mechanisms with limited workspace. Such mechanisms include a 2DOF cartesian robot ([10]), a 3DOF wire-driven mechanism ([12]), a 2DOF 5-bar linkage ([7]), a dual 2DOF 5-bar linkage that redundantly extends [7] into a 3DOF planar mechanism ([8]) and finally a 6DOF parallel redundant mechanism that results in a 3DOF planar interface ([20]).

A potential solution to the limited workspace problem is offered by Mobile Haptic Interfaces (MHIs, [25, 26]). These human-sized interfaces combine a mobile base with a limited-workspace haptic device and follow the locomotion of the operator (thus extending the workspace to the entire walkable floor) in industrial teleoperation and virtual space exploration scenarios. Later studies involving similar devices designed for similar purposes include [5, 16, 34]. More recently, [2, 39] proposed relatively smaller (forearm-sized), link-free desktop MHIs with a strong application focus on upper arm rehabilitation. While these devices certainly mark an improvement towards our goal of building collaborative workspaces composed of many handheld tangible haptic devices, they do not aim to address miniaturizability and inexpensiveness concerns that are absolutely essential for such a platform as ours. Moreover, they are evaluated from a rehabilitation perspective in very specific use cases where corrective performance of the device in path following tasks is measured. For our purposes, evaluation from a more didactic perspective is required where we measure the comprehension of the haptic information that the user is receiving and the sensitivity of this perception, which this article aims to address.

However, most of the device design and control literature focuses on mechanisms that allows to operate within a 3D space for greater workspace versatility; two of the most popular commercial devices are Novint Falcon [24] and PHANToM OMNI [18]. Apart from these, there exists a substantial body of research that is devoted to designing high-end haptic input/output devices for bilateral control of high-end surgical manipulators, as well as haptic-enabled rehabilitation.

Active Tangible Interfaces, namely interfaces that use actuation on its tangible items, also constitute an interesting research area. Studies concerning this modality are mostly of an exploratory nature, suggesting potential applications and differing mainly by their system design. [6, 31] are the first examples in the literature of active tangible interfaces, in the form of 2DOF electromagnetically actuated tokens on a tabletop; [42] later extended this to 3DOF and discussed some haptic interaction possibilities. [37, 21, 33] propose a more conventional approach that is small-size differential drive robots on a graphically active tabletop. [40] showed a programming environment implemented with such an interface. [36] further extended this approach to include tactile feedback. Other less conventional approaches to actuation are ultrasonic proposed by [23] and vibration drive used by [38, 27]. Finally, [3] proposed a zero power haptic device (that harvests power solely from human interaction) that is further explored by [41] briefly as a tangible interface with haptic feedback ability. These studies show existing or potential overlap with robotics and haptics. This potential is still mainly untapped, and there are many more synergies to be found across these fields.

SYSTEM DESIGN

The Cellulo robot is designed with certain constraints that are closely related with its intended educational application focus (discussed in detail in [30]). Namely, our robots must be small enough to be graspable and contain a locomotion system that improves upon the commonly found differential drive (2DOF) in similar active tangible devices to enable instantaneous motion towards any direction when grasped, in order to shift towards a 3DOF haptic device; provide readiness of connectivity with pervasive smart devices (phones, tablets *etc.* that are essential to running our activities) in order to boost acceptance; all the while remaining low cost to not induce economic stress to schools. In this section, we detail the hardware and software components of our robot that ensure its haptic functionality while conforming to the above constraints.

Overview

Our design is composed of a central microcontroller and its peripherals that are part of the *user interface*, *communication & orchestration*, *localization* and *locomotion* submodules, all of which take part in the robot's haptics subsystem. All components come together as seen in Figure 2 within a 3D printed housing designed to be easily graspable and movable. A fully assembled robot measures 75mm from edge to edge, weighs 167.8g and costs about € 126 to prototype including all components and production.

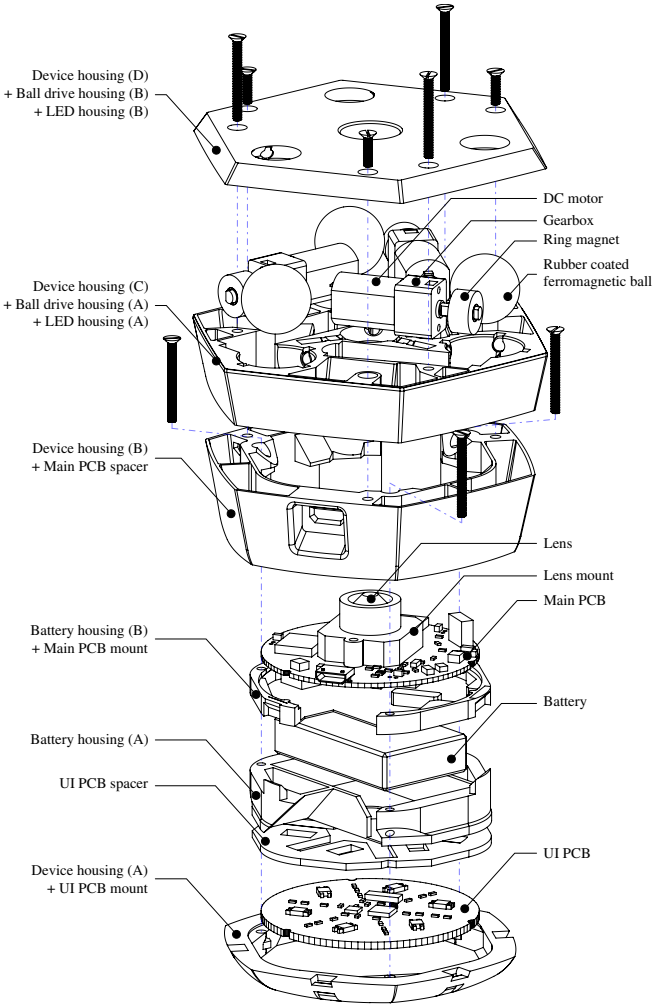

Figure 2. Exploded view of the Cellulo robot, upside-down. Screw routes shown in dashed blue. LEDs, LED cables, motor cables, battery cables and PCB interconnect cable not shown.

User Interface

The robot has 6 full-RGB illuminated capacitive touch buttons on the top surface which can be used individually in key mode (*i.e.* touched/released) or altogether in a primitive *grasp detection* mode. While our approach to detect grasp is similar to those found in [13, 22], we go further by querying the raw values and references sensed at each key by the sensor IC and summing the differences for all 6 keys. We declare the robot *grasped* when this sum exceeds a calibrated threshold value.

Communication & Orchestration

The robot communicates with a consumer tablet (or smartphone, laptop *etc.*) over Bluetooth with binary packets; the robot sends event packets to the tablet (pose changed, key touched *etc.*) and the tablet sends command packets to each robot (track pose, haptic feedback *etc.*). This way, the robots appear as peripherals to the tablet where the activity is orchestrated within a mobile *QtQuick* application; the robots with limited software can thus be used in meaningful and complex scenarios that are programmed within these applications that contain the definition of the "world" to be haptically rendered.

Localization

The robot is able to measure its global absolute pose (x, y, θ) by decoding a deterministic dense optical microdot pattern that is printed on the paper below it. This way, the robot can operate on sheets as large as A0 with desired origin coordinates that can be stitched together indefinitely or used separately, resulting in a practically unlimited workspace composed of single or multiple sheets. This method is detailed in [17] discussing components used, advantages and shortcomings.

Locomotion

The robot is holonomic with 3DOF *i.e.* can (i) Near-instantaneously change direction of motion (also thanks to its low mass), (ii) Start moving in any given direction, (iii) Move with any combination of translational and rotational speed. Its motion is ensured by a ball drive that offers mechanical robustness against user manipulation and compactness in addition to holonomicity. Moreover, using a ball drive instead of a traditional omniwheel drive eliminates vibrations due to discontinuous contact points that may unintentionally be perceived as tactile feedback. Other advantages and shortcomings along with all details of this method are described in [28].

Kinematics & Dynamics

Our arrangement of three 120° apart wheels is very common in holonomic drives and its kinematics are well known. [11, 14, 4] describe the kinematics for ball wheels which requires no special treatment *vs.* more common holonomic drives. The dynamics of our robot was examined (requires slightly more effort due to specific ball drive, is given in the Appendix together with the kinematics for completeness) to obtain the relationship between motor outputs and force/torque applied to the external world (*i.e.* user's hand), allowing us to use this relationship in the design of the motion/haptics controller.

Haptics & Motion Controller Design

Our motion & haptics controller, seen in Figure 3, is essentially a collection of smaller controllers that close the loop from the pose $(x^G, y^G, \theta)_{\text{measured}}$ in the global frame (denoted with G) to the motor outputs U_j. Each of these controllers can be turned on/off, has multiple modes of operation and produces a goal set of velocities (v_x^G, v_y^G, ω) or forces/torque (f_x^G, f_y^G, τ) in the global frame that are converted into motor outputs using the transformations derived in the Appendix. An arbitrary force/torque output $(f_x^G, f_y^G, \tau)_{\text{arbitrary}}$ is also available to be used within a remote loop that runs on the tablet for simulating *e.g.* an arbitrary force/torque field that acts on the robot; this output is switched off when the robot is not grasped in order to prevent involuntary motion. These outputs are summed and sent to the motors as long as the robot is on the paper (*i.e.* not kidnapped) to prevent damage to the robot in typical scenarios where it would fall off the edge of the table. Naturally, the controller is not robust against any combination of these controller outputs; they are explained below along with examples of where the sums are meaningful.

Input/Output

The sensors and actuators on the robot are the camera (used by localization), capacitive touch sensors, motors (M_j, whose outputs are set by the control loop) and visual RGB LEDs. The

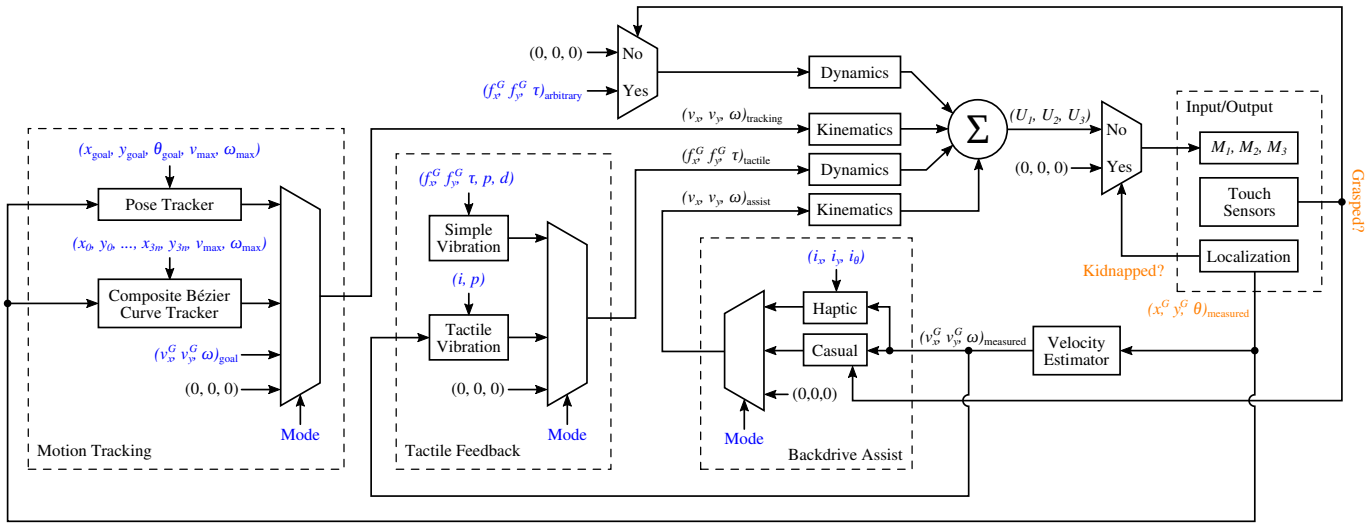

Figure 3. Motion & haptics controller. Values sent by the tablet to the robot are in blue. Values transmitted by the robot to the tablet are in orange.

localization algorithm decodes the pose $(x^G, y^G, \theta)_{\text{measured}}$ in the global frame and whether the robot is kidnapped (*i.e.* is removed from the microdot pattern) with over 93Hz framerate, which dictates the framerate of the entire control loop. A primitive grasp detection method is applied as previously mentioned using the capacitive sensors, *i.e.* by thresholding the sum of the sensor signals. The pose, kidnapped and grasped states are broadcast to the tablet when they change (in orange in Figure 3). The measured pose is then used at each frame to estimate the robot velocity $(v_x^G, v_y^G, \omega)_{\text{measured}}$.

Backdrive Assist

The module controls the friction component of the robot's mechanical impedance by controlling output velocities during motion. A considerable friction component naturally exists and manifests itself as difficulty of moving the robot on the activity sheet due to the friction of the blocked wheels. Presently, there are two backdrive assistance modes to replace this natural component (as much as possible) with a controlled one:

- *Casual mode* is designed to be the *de facto* mode to make the robot easy and comfortable to manipulate, *i.e.* to reduce the natural friction component, by outputting a portion of the measured velocities as goal velocities. These portions (*i.e.* ratios) are tuned to reduce the impedance felt when moving the robot as much as possible while ensuring the controller does not diverge, *i.e.* does not move uncontrollably due to the motion feeding back to its own input. When a grasp is detected, the entire measured velocity is transferred to the output so that the impedance is minimized; the disturbances that would normally cause the assistance to diverge can be stopped by the user with slight effort. The user perceives this as easier motion when the robot is detectably grasped.
- *Haptic mode* is designed to simulate various surfaces that may expose the robot to less or more virtual friction. It transfers parameterized percentages of the measured velocities (with i_x, i_y and i_θ) to the output. Each DOF can be set or disabled individually, resulting in *e.g.* full compliance along x axis and high friction along y. Moreover, negative ratios can also be provided to use the motors to oppose the motion, resulting in the ability to simulate even more friction.

A minor hysteresis was introduced in both modes to enable/disable assist in order to facilitate securing the robot in place and releasing the grasp entirely; the user perceives this as slightly extra inertia when budging the robot.

Tactile Feedback

The module provides oscillatory force feedback and its outputs can be overlaid on the arbitrary force feedback or backdrive assist to provide tactile sensation over kinesthetic sensation, *e.g.* slight vibration over fully compliant backdrive assist to simulate a rugged icy surface. Two generators are available:

- *Simple vibration* provides fixed oscillatory output (with separately controllable force/torque along all DOF, period p and duration d); it can be used *e.g.* as an event indicator. d can be chosen as less than $p/2$ to provide an impulse.
- *Tactile vibration* provides continuous oscillatory output with desired period whose intensities are linearly proportional to the measured robot velocities in the respective DOFs. This generator is used as a very simple model of rough surfaces where more momentum will exert more force on the robot when colliding with the small bumps on the surface, assuming the collision time is constant.

Motion Tracking

The module is used to track one of the following:

- *Any subset of* $(x_{goal}, y_{goal}, \theta_{goal})$ with distinct internal P controllers for each DOF and with maximum linear/angular tracking velocities $v_{\max}, \omega_{\max}$. Desired coordinates can be left out to be controlled by other modules, resulting in *e.g.* fully compliant planar motion (x, y controlled by backdrive assist) while holding a specific orientation (tracking θ).
- *A composite Bézier curve* (*i.e.* cubic Bézier curves connected end-to-end, compliant with the SVG format) described by $3n+1$ control points (denoted by x_k, y_k) and tracked with maximum linear/angular velocities $v_{\max}, \omega_{\max}$.
- *Any subset of an arbitrary* $(v_x^G, v_y^G, \omega)_{goal}$.

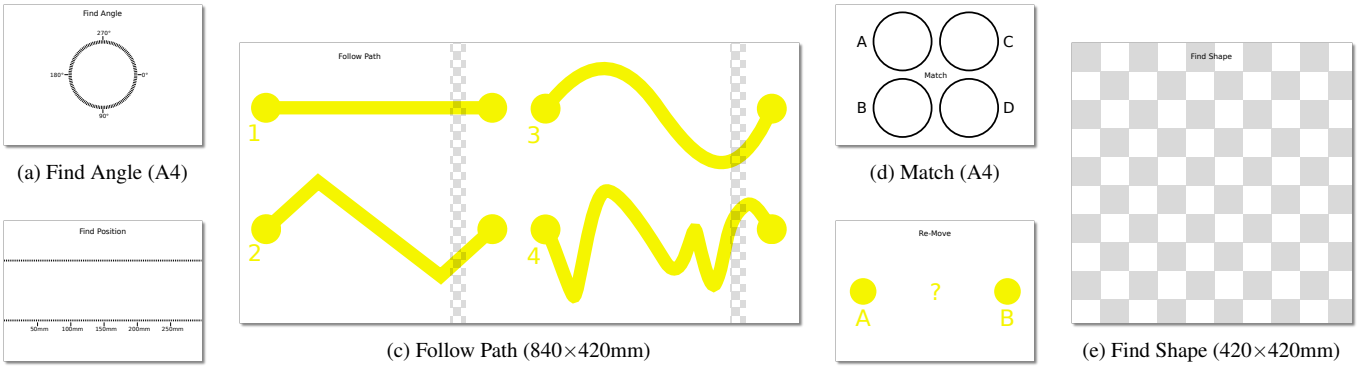

(a) Find Angle (A4)

(b) Find Position (A4)

(c) Follow Path (840×420mm)

(d) Match (A4)

(f) Re-Move (A4)

(e) Find Shape (420×420mm)

Figure 4. Activity sheets for the 6 tasks, scale among sheets is preserved. Microdot pattern omitted. Sheet sizes noted in captions.

EVALUATION & METHODOLOGY

In order to confirm that our design will be useful within our envisioned use cases, we follow a task-based evaluation procedure. The nature of these tasks focuses on measuring haptic perception and manipulation performance where a very specific goal is present in each task (*e.g.* find hidden position by means of haptic feedback). The participant performs each task with the same robot on a distinct printed activity sheet (can be seen in Figure 4) in sequence[1]. A tablet accompanies the tasks where concise information about the current task state and input buttons/choices are displayed.

The order of these tasks were chosen to alternate between motor and perceptive tasks, and to increase in difficulty. Since participants are chosen so that they have not interacted with the Cellulo robots before, the tasks are verbally explained in the beginning if required. Each task is of a functional and non-semantic nature, *i.e.* the participant is not supposed to perceive a virtual environment or associate the feedback with a higher-level concept. With this rationale, we aim to measure the haptic expression and disturbance capabilities of our robots, as well as to confirm their usability (*i.e.* intuitiveness of use) since they are indeed designed to be perceived as consumer devices rather than autonomous or programmable robots.

Task 1: Find Angle

The goal of this task is to *find a hidden orientation* by means of tactile feedback while rotating the robot on the sheet seen in Figure 4a. Haptic backdrive assist is enabled throughout with $(i_x, i_y, i_\theta) = (-0.6, -0.6, 0.6)$, *i.e.* with high linear friction but rotational compliance. If the robot leaves the central area (dashed circle), assist is removed and it is commanded to return to the central area. This way, the robot acts as a "rotary knob" in the center of the activity sheet, conveying a discrete angle with haptic feedback.

Whenever the hidden orientation is crossed, a 30ms torque impulse is given against the direction of crossing. The participant must give an answer that is within $\pm 5°$ of the correct orientation. If correct, the participant advances to the next levels that give less and less intense feedback, calculated as:

$$|\tau_{\text{impulse}}| = \tau_{\max}/2^{\text{level}} \quad (1)$$

where $\tau_{\max}$ denotes the maximum torque output of the robot[2]. The participant is allowed 2 wrong answers in a level except for level 0 which acts as a tutorial (unlimited trials). In this task we measure the participant's sensitivity threshold, where the impulse will start to be indifferentiable from noise. Thanks to this measure we will be able to determine the perceivable interval of torque impulse magnitude.

Task 2: Find Position

The goal of this task is to *find a hidden x coordinate* on the sheet seen in Figure 4b and is very similar to Find Angle. Haptic backdrive assist is enabled throughout with $(i_x, i_y, i_\theta) = (0.7, -0.6, 0.6)$, *i.e.* with high linear friction along the y axis but linear compliance along x axis and rotational compliance for manipulation comfort. If the robot leaves the middle band, assist is removed and it is commanded to return within the band. This way, the robot acts as a "slider knob" conveying a discrete position. Participants are asked to answer with a sensitivity of ± 8mm. The given impulse is as follows:

$$|f^G_{x,\text{impulse}}| = f_{\max}/1.5^{\text{level}} \quad (2)$$

where $f_{\max}$ denotes the maximum force output of the robot[3]. Similarly to the Find Angle task, we measure the participant's sensitivity threshold to determine the perceivable interval of impulse magnitude along a linear axis.

Task 3: Follow Path

The goal of this task is to *move the robot along the paths* on the sheet seen in Figure 4c, and is similar to many path following tasks in the literature. At level 0, the participant moves the robot freely along the paths with casual backdrive assist; the robot moves to the beginning of the next path by itself. At levels 1-3, perturbative impulses are given orthogonal to the path (with random time intervals in between):

$$|f_{\text{impulse}}| = (\text{level}/3) f_{\max}, \quad d_{\text{impulse}} = \text{level} \times 100\text{ms} \quad (3)$$

where $f_{\max}$ again denotes the maximum force output of the robot. The measures for this task are twofold: With level 0, we aim to show that our robots can be manipulated with precision, *i.e.* high position fidelity can be ensured in the presence of

[1] Video showing the sequence of tasks: https://vimeo.com/197382863

[2] Theoretical limit is $\tau_{\max} = 0.0848$Nm, see Appendix

[3] Theoretical limit is $f_{\max} = 1.75$N, see Appendix

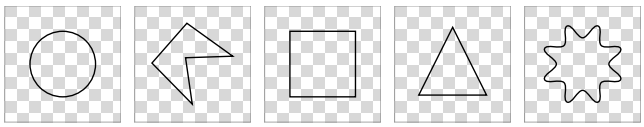

(a) Circle (b) Irregular Polygon (c) Square (d) Triangle (e) Wobbly Circle

Figure 5. Shapes used in Find Shape, also presented to user as choices.

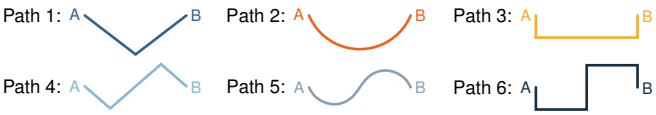

Figure 6. Re-Move paths (not presented to user).

frictional impedance via backdrive assist; with levels 1-3, we aim to measure to what extent our lightweight, low-power and non-grounded robot can disturb the user's motion.

Task 4: Match

The goal of this task is to *find which 2 forces (out of 4) are identical* on the sheet seen in Figure 4d, the robot exerts these constant forces only within the designated circles on the sheet. The two answers are chosen randomly at each level along with one orientation distractor that has same intensity but an orientation that differs from the answer by θ_{distr}, and one intensity distractor that has same the orientation but an intensity that differs from the answer by I_{distr}. These differences are:

$$I_{\text{distr}} = \pm 0.44 f_{\max}/1.2^{\text{level}}, \quad \theta_{\text{distr}} = \pm 180°/1.2^{\text{level}} \qquad (4)$$

In other words, the distractors become more and more similar to the answers as levels progress. Here, it should be noted that the dead band described in the dynamics analysis (see Appendix) is also used extensively; the robot outputs significant amounts of audible noise when the motors are driven, whose intensity and frequency may be proportional to the motor outputs. This element was left in the experiment as it is to be expected during normal use, and may be beneficial to the task.

With this task, we aim to measure to what extent the user can differentiate the intensity and orientation of forces conveyed by the robot, thus obtaining a general understanding of the force feedback resolution with our robots.

Task 5: Find Shape

The goal of this task is to *find which of the 2D closed curves* (given in Figure 5) is hidden on the sheet seen in Figure 4e. The robot is used as a "scanner" (with casual backdrive assist) to probe the randomly selected shape that has a 10mm-thick border on which the robot gives tactile vibration with intensity:

$$i_{\text{tactile}} = 3.0/1.5^{level} \qquad (5)$$

The participant is allowed only 1 wrong choice. With this task, we attempt to examine to which extent our robots are able to let the user feel (or rather discover) 2D curves through haptic feedback even though they are inherently point-like objects.

Task 6: Re-Move

The goal of this task is to *feel the trajectory of the robot and repeat it* on the sheet seen in Figure 4f. The participant is asked

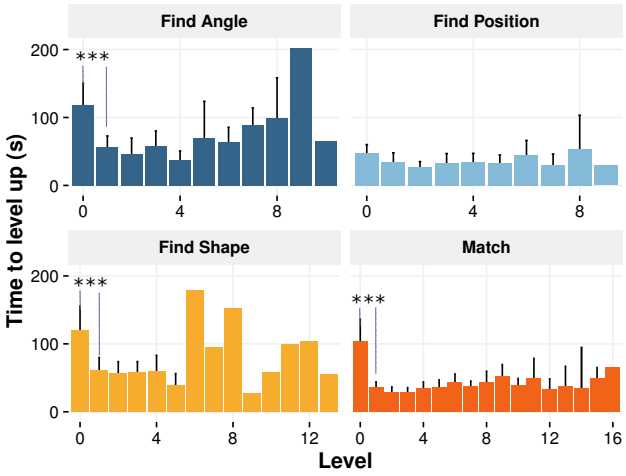

Figure 7. Average time taken by participants to complete each level for Find Angle, Find Position, Find Shape and Match.

to *close their eyes* and grasp the robot which starts to move along one of the paths seen in Figure 6 and goes back to the start. The participant then moves the robot along the recalled path. Each of the 6 paths are performed in random order with $v_{\max} = 75$mm/s (level 0), and $v_{\max} = 150$mm/s (level 1). Similar to Follow Path, we aim to measure the fidelity to the actual path, but with all visual components removed. With this, we simulate scenarios where the user may be obliged to look elsewhere while interacting with the robot whose motion must be perceived and remembered.

RESULTS & DISCUSSION

25 participants (10F and 15M, 31.7±7.48 years old, 4% left-handed, 40% used robots in daily life before, including robotic vacuum cleaners) were recruited to perform all the tasks. None of these participants had any prior experience with our platform. Due to the repetitive nature of the tasks, the experiment was performed exclusively with adults to not introduce excessive fatigue effects into our measures (between 30min and 50min long depending on the participant). It is known that fine motor skills (including haptic perception) are achieved by the age of 7 and only some of these (such as handwriting and drawing) continue to be refined into late childhood ([32]), suggesting that our evaluation should be repeatable with late primary school children without significant loss of accuracy on results. Here, we discuss our findings (through the measures from tasks described above) that shed light on the main findings in haptic rendering performed by our robots.

Self Acquisition - User Friendliness

Among the tasks the participants performed, some are level-based and require a correct answer (orientation, position, shape, matching forces) to advance to the next level. Measuring the time it takes to advance to the next level in these tasks (seen in Figure 7) reveals the evolution pattern of the difficulty across levels: The time spent drops for all tasks after level 0, stays similar for a number of levels and then generally tends to increase as it requires more and more time due to the increasing sensitivity required to find the correct answer. Paired t-tests (within subject) between levels 0 and 1

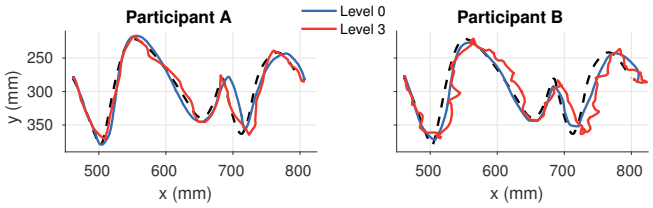

Figure 8. Sample paths performed in Follow Path by one of the most successful participants (left) and one of the least successful participants (right) in counteracting disturbance.

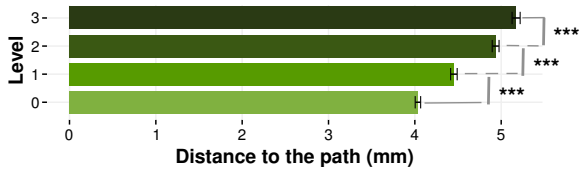

Figure 9. Fidelities to the actual paths in Follow Path with different levels of haptic disturbance (error bars denote 98% confidence intervals).

confirm that this drop is significant except for Find Position[4] ($p = 0.001$, $p = 0.12$, $p = 0.0001$, $p = 0.005$ for Find Angle, Find Position, Match and Find Shape respectively). These trends evidence that level 0 acted as a tutorial level that lasted about 2 minutes and "trained" the users (who had no prior experience with our platform) while performing the task itself without assistance from experimenters: This shows that our platform, within such tasks, is approachable and user friendly.

Disturbative Output

Follow Path aimed to determine the robot's disturbative capacities on the participant having to follow a variety of paths seen in Figure 4c (straight, piecewise straight, smooth with single inflection point and irregular smooth with many inflection points). Example performances by two participants in level 0 (no disturbance) and level 3 (maximum disturbance) on the irregular path is shown in Figure 8. As shown by Figure 9, we observed significant influence of disturbance on the participants' precisions in following the paths. Differences between consecutive levels were all found to be significant (confidence intervals at 98%):

$$\textit{L0 - L1: } t(129540) = -21.0, p < 0.001, \mathrm{CI} = [-0.46, -0.37]$$
$$\textit{L1 - L2: } t(143490) = -21.8, p < 0.001, \mathrm{CI} = [-0.53, -0.43]$$
$$\textit{L2 - L3: } t(147930) = -9.53, p < 0.001, \mathrm{CI} = [-0.30, -0.18]$$

On average, the robot is able to add about 28% error (at maximum output, level 3) to the user's natural error level (at no output, level 0) which can be tuned with adjusting the output. Of course, these outputs are limited to be informative and are not on par with high levels of human power output (about two orders of magnitude difference). In other words, if the user had full knowledge of the incoming disturbative output from a single robot, they would be able to counteract with ease.

Backdrivability in Following a Visual 2D Path

Follow Path was also used to measure participants' precision to follow a path under normal circumstances with casual backdrive assist At level 0 (no disturbance), the distance to the actual path was found to be 4.04 mm on average. This level of error corresponds to between 1.1% and 0.51% of the paths' entire lengths and to 5.4% of the robot's body length, evidencing that it is possible to precisely backdrive the robot during normal use with active backdrive assist.

[4]This may be explained by the very similar nature of this task as the preceding task (Find Angle) and its already low level 0 completion time, which hints at transfer of learning.

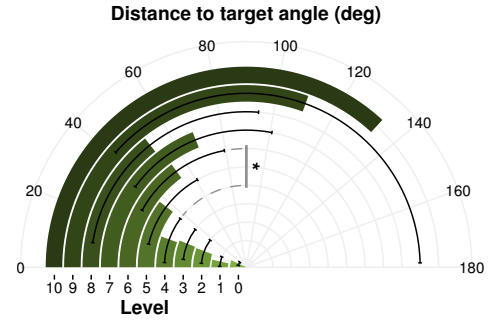

Figure 10. Participants' average distance to the correct angle in Find Angle, error bars denote standard deviation.

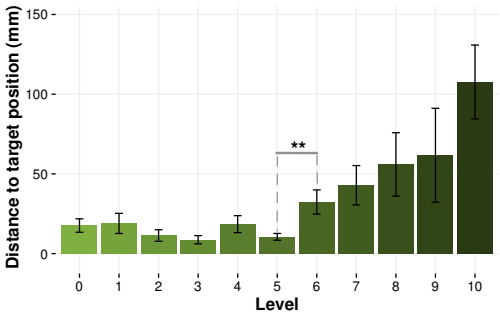

Figure 11. Participants' average distance to the correct position in Find Position, error bars denote standard deviation.

Expressing Discrete Orientations & Positions

Find Angle and Find Position tasks had participants find orientations and horizontal positions using only haptic feedback, whose intensity decreased along the levels. Figures 10 and 11 show decreasing trends in participants' precisions (*i.e.* distances of given answers to the actual orientation/position) as the haptic feedback becomes weaker. In both tasks, comparing these precisions across consecutive levels reveals the locations of the hypothesized sensitivity thresholds. For angles, this corresponds to somewhere between level 4 ($19.82° \pm 41.07°$) and level 6 ($54.01° \pm 64.11°$) whose difference is significant (Welch's $t(44.48) = -2.32, p = 0.0250$). For positions, this corresponds to somewhere between level 5 ($10.52\text{mm} \pm 12.25\text{mm}$) and level 6 ($32.36\text{mm} \pm 44.85\text{mm}$) whose difference is significant (Welch's $t(39.33) = -2.77, p = 0.008$). These thresholds definitively mark the points where users lose precision and possibly lose comfort in perceiving the haptic feedback. More data with more sensitivity resolution may reveal more accurate threshold locations. From a success perspective, all participants except one[5] reached at least level 2 in Find Angle while all participants reached at least level 4 in Find Position.

[5]This participant was observed to show exceptional reluctance to the device at first (as this was the first task) but then overcame this reluctance and reached level 7 in Find Position.

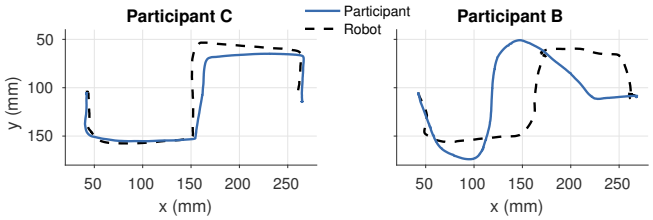

Figure 12. Sample paths performed in Re-Move by one of the most successful participants (left) and one of the least successful participants (right). Since robots are grasped when performing, the reference paths (dashed) may be imperfect.

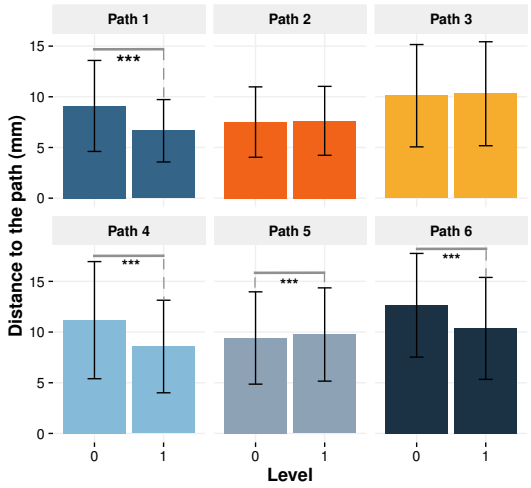

Figure 13. Participants' average precisions moving the robot along 6 different paths with 2 levels of velocity in Task 6 (Re-Move), error bars denote standard deviation.

Expressing 2D Paths Purely Kinesthetically

Re-Move had participants follow a 2D path that was displayed by the motion of the robot with no visual feedback; Figure 12 shows examples of the Path 6 performed by two participants. Two velocity levels were tested as this task also involved the successful recall of the path while it was performed by the participant. Average precisions with respect to each path (seen in Figure 13) revealed that the performance increased significantly for paths 1, 4 and 6 (piecewise straight paths) and decreased significantly for path 5 (smooth path with one inflection point). This suggests that straight paths may be more difficult to recall while smooth paths with enough inflection points may be distorted more by faster motion, as the participants followed the actual path that was enacted by the robot. A more focused study is necessary to confirm these claims.

When the worse of the average performances among the two levels are considered, participants were able to achieve errors of 3.33%, 2.76%, 3.31%, 3.89%, 3.53% and 3.10% of the total path lengths for paths 1, 2, 3, 4, 5 and 6 respectively; these correspond to 12.1%, 10.2%, 13.7%, 14.9%, 12.9% and 16.8% of the robot's body length, evidencing the ability of the robot to convey a variety of paths with only kinesthetic feedback.

Expressing Closed 2D Curves

Find Shape had participants discover which of the five shapes was hidden on the paper sheet using tactile feedback given by the contour of the shape. No significant difference was found between the shapes in terms of performance. We found that participants were generally not performant: It was observed that casually exploring the activity sheet did not reveal the shape for most participants, and that it was necessary to develop systematic scan strategies that was achieved by only few participants during the short duration they spent in the activity. This may indicate that a continuous long-distance rendering of the border (force towards/away from the border) may be a better approach to expressing 2D curves than a binary (haptic feedback on/off) border exploration method.

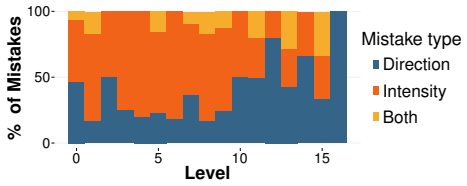

Figure 14. Types of mistakes according to level in the Match.

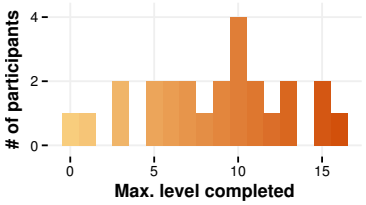

Figure 15. Number of participants that completed each level in Match.

Expressing Stationary Forces

Match aimed to evaluate if participants were able to differentiate forces that were more and more similar as levels progressed. With the given answers, we separately measured how many wrong answers were given due to direction or due to intensity, shown in Figure 14. This shows a trend in more mistakes due to intensity compared to direction (especially in lower levels): It was observed that many participants discovered that they could use the robot's motion inside the small operational area (10mm diameter circle in the center of each area) while lightly grasping it and letting it move to observe the direction of the force, suggesting why less direction mistakes may have been made. Moreover, as mentioned in the task description, the audible noise generated by the motors is potentially indicative of the applied force. On one hand, this modality complements the haptic feedback and may enhance the force perception. On the other hand, it may be unusable or inaccessible in the presence of many robots or a noisy environment.

From a success perspective, Figure 15 shows the number of participants who reached each level, revealing a spectrum of perception resolution. All but 4 participants completed at least level 5, denoting a capability in differentiating at least 17.7% intensity (compared to maximum output) and 72.3° orientation. For these few participants who did not perform as well, more training than what was available in the experiment may be necessary to improve perception performance. When the median is considered, the majority of the participants completed at least level 9, denoting 8.53% intensity (compared to maximum output) and 34.9° orientation differentiation capability.

Summary of Findings

Here, we summarize the findings from our evaluation procedure that address our aforementioned research challenges:

- For users without prior experience, our platform is easy and intuitive to start using; for tasks such as the ones tested, about 2 minutes of familiarization is enough on average.
- Up to 28% disturbance can be added to the precision of motion when the robot is being manipulated.
- Despite high internal friction, the robot can be back-driven with active assistance with up to 5.4% body lengths (4.04mm) precision on average.
- Angles and positions can be conveyed with impulses as low as 1.56%-6.25% of $\tau_{\max}$ and 8.78%-13.2% of $f_{\max}$.
- Paths can be kinesthetically conveyed and are repeatable with 2.76% to 3.89% path length precision on average.
- 2D curves on a plane cannot be conveyed efficiently when the robot is used as a point scanner.
- About 8.53% force magnitude (with respect to $f_{\max}$) and 34.9° force direction can be distinguished by the majority of individuals, but with limitations (presence of auditory feedback and small scale displacement).

Towards Haptic-Enabled Learning Activities

Finally, we discuss the contribution of the design and evaluation done in this article to the Cellulo workflow; namely building educative activities with haptic and tangible interaction elements in order to achieve imaginative, engaging and effective learning situations. Importantly, the integration of haptic interaction into activities must be easy, natural and efficient; the reasons for which include maximizing the benefit from the (essential) active participation of teachers in this design process, who do not necessarily possess technical skills. For this reason, we aimed to evaluate our platform in terms of haptic interaction "atoms" (built around the basic DOF found in our interaction space) that can be used as on-demand building blocks. Although this may not be the optimal approach to benefit all HCI applications in general, we believe it is favorable for facilitating developer-designer-teacher communication in order to improve the co-design process of activities.

With these building blocks, we believe a wide variety of scenarios can be implemented. For instance, robots may represent interconnected gears that "click" (as in Find Angle) when a turn is completed to lead the learners to the relationship between the number of teeth and number of turns. Another activity taking place on the cartesian plane may involve an autonomous robot enacting a path and another robot that must be moved (as in Follow Path) in the symmetric path with respect to a given axis in order to instruct in geometrical symmetry. In yet another scenario, robots may stand for various chemical elements in given molecular bonds where the strength of the force resulting from the bonds must be felt (as in Match) in order to teach unequal levels of electronegativity found in elements. On the other hand, our set of interaction atoms is certainly not exhaustive, nor do we aim to restrict the interactions in an activity to exclusively haptic. We imagine that our activities are enhanced by haptics (that is to be perceived as an added value) and may include phases where paper-based tangible interaction or only observation may be prevalent.

CONCLUSION

In this article, we presented our haptic-enabled handheld mobile robot that is novel in bringing together handheld robots (*i.e.* active tangible items) and full planar haptic feedback capability. We showed its usability in a number of tasks and extracted related performance measures. We conclude with our design's shortcomings, planned future work and outlook.

Shortcomings & Future Work

Perhaps the most significant shortcoming of our design is that it essentially does not guarantee precision on its haptic output since it's not a grounded mechanism; it is supposed to be removed from the activity sheet and placed back on the same/other activity sheet(s) during normal use as a tangible item. Therefore, the design of the activities that will use our robot should actively take this into account and be designed such that they tolerate low precision in the haptic output. A second shortcoming is that the robot operates by nature on a plane, therefore is only suitable to convey planar and/or rotational haptic feedback.

Since the robot is not equipped with force/torque sensors yet, closed-loop control of the force/torque output to the user's hand cannot be performed. This restricts the control to an open loop where the grasp presence is measured by capacitive touch sensors which does not guarantee the actual transmission of force/torque. In addition, the capacitive touch sensors are sensitive to temperature and moisture that introduce an undesirable hysteresis in the grasped/released state, failing to detect the release after long grasps. We will attempt to mitigate these problems with force/torque sensing on the outer shell of the robot, for which an array of sensors such as [35] is a promising candidate. Furthermore, several simplifications were deemed appropriate in the dynamics analysis of the robot thanks to its light weight. For better interaction performance, a full analysis is required which is left as future work.

Outlook

The long term goal of the Cellulo project is to show the utility of the platform as a practical educative tool (discussed in [30]) but other potential applications exist beyond education. As the robots are precisely localized and are capable of haptic output, a particularly appealing application is interfaces for the visually impaired (both learners and users), such as interactive geographical maps (*e.g.* [9] augmented with haptic feedback). From another perspective, at-home rehabilitation of upper limbs is also appealing as a use case (in the same vein as [2, 39]): Although Cellulo is too lightweight to perform as a "corrective coach", it goes further in portability and lowering cost and may be more easily accepted if the rehabilitative activities are built around gamifying regular exercises. Besides rehabilitation, the multiplicity and paper-basedness of Cellulo may be exploited to build "board games" with haptic-enabled tangible elements (pieces as well as controllers) that may autonomously move or be moved by players.

ACKNOWLEDGEMENTS

We would like to thank the Swiss National Science Foundation for supporting this project through the National Centre of Competence in Research Robotics.

APPENDIX

Given that v_j^L denotes the j^{th} wheel's velocity in the local frame, v_x^G, v_y^G, ω denote the linear and angular robot velocities in the global frame, the inverse kinematics of the robot are given as:

$$\begin{pmatrix} v_1^L \\ v_2^L \\ v_3^L \end{pmatrix} = K^{-1} R(-\theta) \begin{pmatrix} v_x^G \\ v_y^G \\ \omega \end{pmatrix} \tag{6}$$

$$K^{-1} = \begin{pmatrix} -1 & 0 & D \\ \frac{1}{2} & -\frac{\sqrt{3}}{2} & D \\ \frac{1}{2} & \frac{\sqrt{3}}{2} & D \end{pmatrix}; \quad R(\theta) = \begin{pmatrix} \cos\theta & -\sin\theta & 0 \\ \sin\theta & \cos\theta & 0 \\ 0 & 0 & 1 \end{pmatrix} \tag{7}$$

where D is the center to wheel distance (28mm for our robot). [19] gives the dynamics of an omniwheeled robot; the transmission from the ground forces to robot forces and torque hold in our case as well (assuming a similar notation as velocities):

$$\begin{pmatrix} f_1^L \\ f_2^L \\ f_3^L \end{pmatrix} = C^{-1} R(-\theta) \begin{pmatrix} f_x^G \\ f_y^G \\ \tau \end{pmatrix} = C^{-1} R(-\theta) \begin{pmatrix} m a_x^G \\ m a_y^G \\ I_z \alpha \end{pmatrix} \tag{8}$$

$$C^{-1} = \begin{pmatrix} -2/3 & 0 & 1/(3D) \\ 1/3 & -\sqrt{3}/3 & 1/(3D) \\ 1/3 & \sqrt{3}/3 & 1/(3D) \end{pmatrix} \tag{9}$$

Considering that the robot orientation is known at all times in our case (given by onboard global localization), the above equations can be used to calculate the necessary wheel forces in order to obtain the desired force/torque output from the robot. For each of the 3 DC motors:

$$\tau_j = c_u U_j - c_\omega \omega_j \tag{10}$$

where U_j, ω_j and τ_j are the output (*i.e.* voltage), angular velocity and torque of the j^{th} motor respectively and c_u, c_ω are positive constants. This can also be expressed as

$$\tau_j = c_u U_j - c_v v_j^L \tag{11}$$

assuming no slip between the drive roller-wheel and wheel-ground contacts where c_v is another positive constant. It is previously shown in [28] that output wheel forces for such a drive as ours can be expressed as a discontinuous piecewise linear function of the motor torque. Simplifying it further by ignoring the degenerate state (entered by a narrow torque band) allows us to express this linear dependency in only two regions that depend on the direction of the wheel's motion:

$$\tau_j = c_f(\text{sgn}(v_j^L)) f_j^L + c(\text{sgn}(v_j^L)) \tag{12}$$

where $c_f(s)$, $c(s)$ are dual constants that take two different values. $c_f(s)$ represents the force-torque coupling and therefore is always positive while $c(s)$ represents friction and is the same sign as s, resulting in the additional torque requirement. Equating Equations 11 and 12:

$$c_u U_j - c_v v_j^L = c_f(\text{sgn}(v_j^L)) f_j^L + c(\text{sgn}(v_j^L)) \tag{13}$$

At this point, we make the further simplification that the robot's mass and moment of inertia are negligible so that it can accelerate/decelerate instantly from the user's point of view. It was empirically measured that the robot can reach its maximum velocity (about 185mm/s) in 0.23s and maximum angular velocity (about 7.2rad/s) in 0.40s when the motors are driven with full output, justifying this simplification. Then Equation 8 is approximately equal to the zero vector, making the wheel-ground forces approximately zero:

$$c_u U_j \simeq c_v v_j^L + c(\text{sgn}(v_j^L)) \tag{14}$$

Plugging in Equation 6 and dividing by c_u:

$$\begin{pmatrix} U_1 \\ U_2 \\ U_3 \end{pmatrix} \simeq \hat{c_v} K^{-1} R(-\theta) \begin{pmatrix} v_x^G \\ v_y^G \\ \omega \end{pmatrix} + \begin{pmatrix} \hat{c}(\text{sgn}(v_1^L)) \\ \hat{c}(\text{sgn}(v_2^L)) \\ \hat{c}(\text{sgn}(v_3^L)) \end{pmatrix} \tag{15}$$

Here, $\hat{c_v} = c_v/c_u$ and $\hat{c}(s) = c(s)/c_u$ where c_v and c_u are to be calibrated. This allows calculating the motor outputs for the desired isolated robot motion.

In the presence of user interaction however, the robot is likely to be blocked in place. In this case, the drive roller-wheel contact will be broken with enough motor torque. Under ideal conditions given in [28] and ignoring internal friction, $f_{j,\max}^L = 1.01\text{N}$ can be transmitted, resulting in a theoretical maximum output of $f_{x,y,\max}^G = 1.75\text{N}$ and $\tau_{\max} = 0.0848\text{Nm}$. $f_{x,y,\max}^G$ was empirically observed to be $0.78\pm0.10\text{N}$ (measured from all 6 sides) when the robot is not grasped and to be up to $1.99\pm0.21\text{N}$ with a 500g weight on top of the robot simulating a strong grasp. Until the contact is broken, the motors are stalled and their torques are transmitted directly to the ground after some portion is lost to internal friction. Equation 11 and 12 now become:

$$\tau_j = c_u U_j \quad \text{and} \quad \tau_j = c_f' f_j^L + c'(\text{sgn}(f_j^L)) \tag{16}$$

where c_f' and $c'(s)$ now depend on the exact configuration that the robot is grasped in (*i.e.* whether the wheels are in *forward*, *backward* or intermediate positions) and cannot be determined by the current hardware, resulting in additional loss of precision. $c'(s)$ again represents the additional torque lost to friction (now static) and is the same sign as τ_j which is the same direction as f_j^L. Equating the above two equations and plugging them into Equation 8:

$$\begin{pmatrix} U_1 \\ U_2 \\ U_3 \end{pmatrix} = \hat{c_f}' C^{-1} R(-\theta) \begin{pmatrix} f_x^G \\ f_y^G \\ \tau \end{pmatrix} + \begin{pmatrix} \hat{c}'(\text{sgn}(f_1^L)) \\ \hat{c}'(\text{sgn}(f_2^L)) \\ \hat{c}'(\text{sgn}(f_3^L)) \end{pmatrix} \tag{17}$$

Here, $\hat{c_f}' = c_f'/c_u$ and $\hat{c}'(s) = c'(s)/c_u$ where c_u is the same as before and c_f' and $c'(s)$ are to be calibrated with average values. After $f_{\max}$ (*i.e.* when the roller-wheel contact is broken), the roller will apply a kinetic friction force to the wheel that will be transmitted to the ground, resulting in the clamping of the force applied to the robot at the wheel level. Considering the nominal stall torque of our motors (0.0348Nm at 3.7V), this maximum force corresponds to only 14% of the drive's (theoretical, per wheel) capacity. Therefore, the force output can only be controlled in this narrow band when the robot is blocked and the outside dead band is reserved for motion.

REFERENCES

1. Motoyuki Akamatsu and Sigeru Sato. 1994. A multi-modal mouse with tactile and force feedback. *International Journal of Human-Computer Studies* 40, 3 (1994), 443–453. DOI: http://dx.doi.org/10.1006/ijhc.1994.1020
2. Carlo Alberto Avizzano, Massimo Satler, and Emanuele Ruffaldi. 2014. Portable Haptic Interface with Omni-Directional Movement and Force Capability. *IEEE Transactions on Haptics* 7, 2 (2014), 110–120. DOI: http://dx.doi.org/10.1109/TOH.2014.2310462
3. Akash Badshah, Sidhant Gupta, Gabe Cohn, Nicolas Villar, Steve Hodges, and Shwetak N. Patel. 2011. Interactive Generator: A Self-powered Haptic Feedback Device. In *Proceedings of the SIGCHI Conference on Human Factors in Computing Systems (CHI)*. 2051–2054. DOI:http://dx.doi.org/10.1145/1978942.1979240
4. David M. Ball, Chris F. Lehnert, and Gordon F. Wyeth. 2010. A Practical Implementation of a Continuous Isotropic Spherical Omnidirectional Drive. In *Proceedings of the 2010 IEEE International Conference on Robotics and Automation (ICRA)*. 3775–3780. DOI: http://dx.doi.org/10.1109/ROBOT.2010.5509645
5. Federico Barbagli, Alessandro Formaglio, M. Franzini, Antonio Giannitrapani, and Domenico Prattichizzo. 2006. An Experimental Study of the Limitations of Mobile Haptic Interfaces. In *Experimental Robotics IX: The 9th International Symposium on Experimental Robotics*. 533–542. DOI:http://dx.doi.org/10.1007/11552246_51
6. Scott Brave, Hiroshi Ishii, and Andrew Dahley. 1998. Tangible Interfaces for Remote Collaboration and Communication. In *Proceedings of the 1998 ACM Conference on Computer Supported Cooperative Work*. 169–178. DOI:http://dx.doi.org/10.1145/289444.289491
7. Gianni Campion, Qi Wang, and Vincent Hayward. 2005. The Pantograph Mk-II: A Haptic Instrument. In *Proceedings of the 2005 IEEE/RSJ International Conference on Intelligent Robots and Systems (IROS)*. 45–58. DOI: http://dx.doi.org/10.1109/IROS.2005.1545066
8. Daniela Constantinescu, Icarus Chau, Simon P. DiMaio, Luca Filipozzi, Septimiu E. Salcudean, and Farhad Ghassemi. 2000. Haptic Rendering of Planar Rigid-Body Motion using a Redundant Parallel Mechanism. In *Proceedings of the 2000 IEEE International Conference on Robotics and Automation (ICRA)*, Vol. 3. 2440–2445. DOI:http://dx.doi.org/10.1109/ROBOT.2000.846393
9. Julie Ducasse, Marc Macé, Marcos Serrano, and Christophe Jouffrais. 2016. Tangible Reels: Construction and Exploration of Tangible Maps by Visually Impaired Users. In *Proceedings of the 2016 CHI Conference on Human Factors in Computing Systems*. DOI: http://dx.doi.org/10.1145/2858036.2858058
10. Randy E. Ellis, Ossama M. Ismaeil, and Michael G. Lipsett. 1996. Design and evaluation of a high-performance haptic interface. *Robotica* 14, 03 (1996), 321–327. DOI: http://dx.doi.org/10.1017/S0263574700019639
11. Laurent Ferrière and Benoît Raucent. 1998. ROLLMOBS, a new universal wheel concept. In *Proceedings of the 1998 IEEE International Conference on Robotics and Automation (ICRA)*, Vol. 3. 1877–1882. DOI: http://dx.doi.org/10.1109/ROBOT.1998.680516
12. Paolo Gallina, Giulio Rosati, and Aldo Rossi. 2001. 3-d.o.f. Wire Driven Planar Haptic Interface. *Journal of Intelligent and Robotic Systems* 32, 1 (2001), 23–36. DOI: http://dx.doi.org/10.1023/A:1012095609866
13. Steven Gelineck, Dan Overholt, Morten Büchert, and Jesper Andersen. 2013. Towards an Interface for Music Mixing based on Smart Tangibles and Multitouch. In *Proceedings of the International Conference on New Interfaces for Musical Expression*. 180–185. http://nime.org/proceedings/2013/nime2013_206.pdf
14. Hashem Ghariblu, Ali Moharrami, and Benham Ghalamchi. 2011. Design and Prototyping of Autonomous Ball Wheel Mobile Robots. In *Mobile Robots - Current Trends*. InTech Open Access Publisher. DOI:http://dx.doi.org/10.5772/25936
15. Andrew H. Gosline, Gianni Campion, and Vincent Hayward. 2006. On The Use of Eddy Current Brakes as Tunable, Fast Turn-On Viscous Dampers For Haptic Rendering. In *Proceedings of Eurohaptics*. 229–234. http://www.cim.mcgill.ca/~haptic/devices/pub/AG-ET-AL-EH-06.pdf
16. Kyung-Lyong Han, Oh Kyu Choi, In Lee, Inwook Hwang, Jin S. Lee, and Seungmoon Choi. 2008. Design and Control of Omni-Directional Mobile Robot for Mobile Haptic Interface. In *Control, Automation and Systems, 2008. ICCAS 2008. International Conference on*. 1290–1295. DOI: http://dx.doi.org/10.1109/ICCAS.2008.4694349
17. Lukas O. Hostettler, Ayberk Özgür, Séverin Lemaignan, Pierre Dillenbourg, and Francesco Mondada. 2016. Real-Time High-Accuracy 2D Localization with Structured Patterns. In *Proceedings of the 2016 IEEE International Conference on Robotics and Automation (ICRA)*. 4536–4543. DOI: http://dx.doi.org/10.1109/ICRA.2016.7487653
18. Alejandro Jarillo-Silva, Omar A. Domínguez-Ramírez, Vicente Parra-Vega, and J. Patricio Ordaz-Oliver. 2009. PHANToM OMNI Haptic Device: Kinematic and Manipulability. In *Proceedings of the Electronics, Robotics and Automotive Mechanics Conference, 2009 (CERMA)*. 193–198. DOI: http://dx.doi.org/10.1109/CERMA.2009.55
19. Tamás Kalmár-Nagy, Raffaello D'Andrea, and Pritam Ganguly. 2004. Near-optimal dynamic trajectory generation and control of an omnidirectional vehicle. *Robotics and Autonomous Systems* 46, 1 (2004), 47–64. DOI:http://dx.doi.org/10.1016/j.robot.2003.10.003

20. Tae-Ju Kim, Byung-Ju Yi, and Il Hong Suh. 2004. Load Distribution Algorithms and Experimentation For a Redundantly Actuated, Singularity-Free 3-DOF Parallel Haptic Device. In *Proceedings of the 2004 IEEE/RSJ International Conference onIntelligent Robots and Systems (IROS)*, Vol. 3. 2899–2904. DOI: http://dx.doi.org/10.1109/IROS.2004.1389849

21. Aleksander Krzywinski, Haipeng Mi, Weiqin Chen, and Masanori Sugimoto. 2009. RoboTable: A Tabletop Framework for Tangible Interaction with Robots in a Mixed Reality. In *Proceedings of the International Conference on Advances in Computer Enterntainment Technology*. 107–114. DOI: http://dx.doi.org/10.1145/1690388.1690407

22. Mathieu Le Goc, Pierre Dragicevic, Samuel Huron, Jeremy Boy, and Jean-Daniel Fekete. 2015. SmartTokens: Embedding Motion and Grip Sensing in Small Tangible Objects. In *Proceedings of the 28th Annual ACM Symposium on User Interface Software & Technology*. 357–362. DOI: http://dx.doi.org/10.1145/2807442.2807488

23. Mark Marshall, Thomas Carter, Jason Alexander, and Sriram Subramanian. 2012. Ultra-tangibles: Creating Movable Tangible Objects on Interactive Tables. In *Proceedings of the SIGCHI Conference on Human Factors in Computing Systems (CHI)*. 2185–2188. DOI: http://dx.doi.org/10.1145/2207676.2208370

24. Steven Martin and Nick Hillier. 2009. Characterisation of the Novint Falcon Haptic Device for Application as a Robot Manipulator. In *Proceedings of the Australasian Conference on Robotics and Automation (ACRA)*. 291–292. http://www.araa.asn.au/acra/acra2009/papers/pap127s1.pdf

25. Norbert Nitzsche, Uwe D. Hanebeck, and Günther Schmidt. 2001. Mobile Haptic Interaction with Extended Real or Virtual Environments. In *Proceedings 10th IEEE International Workshop on Robot and Human Interactive Communication (ROMAN 2001)*. 313–318. DOI: http://dx.doi.org/10.1109/ROMAN.2001.981921

26. Norbert Nitzsche, Uwe D. Hanebeck, and Günther Schmidt. 2003. Design Issues of Mobile Haptic Interfaces. *Journal of Robotic Systems* 20, 9 (2003), 549–556. DOI:http://dx.doi.org/10.1002/rob.10105

27. Diana Nowacka, Karim Ladha, Nils Y. Hammerla, Daniel Jackson, Cassim Ladha, Enrico Rukzio, and Patrick Olivier. 2013. Touchbugs: Actuated Tangibles on Multi-touch Tables. In *Proceedings of the SIGCHI Conference on Human Factors in Computing Systems (CHI)*. 759–762. DOI: http://dx.doi.org/10.1145/2470654.2470761

28. Ayberk Özgür, Wafa Johal, and Pierre Dillenbourg. 2016. Permanent Magnet-Assisted Omnidirectional Ball Drive. In *Proceedings of the 2016 IEEE/RSJ International Conference on Intelligent Robots and Systems (IROS)*. DOI:http://dx.doi.org/10.1109/IROS.2016.7759180

29. Ayberk Özgür, Wafa Johal, Francesco Mondada, and Pierre Dillenbourg. 2017a. Windfield: Learning Wind Meteorology with Handheld Haptic Robots. In *HRI '17: ACM/IEEE International Conference on Human-Robot Interaction Proceedings*. DOI: http://dx.doi.org/10.1145/2909824.3020231

30. Ayberk Özgür, Séverin Lemaignan, Wafa Johal, Maria Beltran, Manon Briod, Léa Pereyre, Francesco Mondada, and Pierre Dillenbourg. 2017b. Cellulo: Versatile Handheld Robots for Education. In *HRI '17: ACM/IEEE International Conference on Human-Robot Interaction Proceedings*. DOI: http://dx.doi.org/10.1145/2909824.3020247

31. Gian Pangaro, Dan Maynes-Aminzade, and Hiroshi Ishii. 2002. The Actuated Workbench: Computer-controlled Actuation in Tabletop Tangible Interfaces. In *Proceedings of the 15th Annual ACM Symposium on User Interface Software and Technology*. 181–190. DOI: http://dx.doi.org/10.1145/571985.572011

32. V. Gregory Payne and Larry D. Isaacs. 2012. *Human Motor Development: A Lifespan Approach* (8 ed.). McGraw-Hill. http://scholarworks.sjsu.edu/faculty_books/1

33. Esben Warming Pedersen and Kasper Hornbæk. 2011. Tangible Bots: Interaction with Active Tangibles in Tabletop Interfaces. In *Proceedings of the SIGCHI Conference on Human Factors in Computing Systems (CHI)*. 2975–2984. DOI: http://dx.doi.org/10.1145/1978942.1979384

34. Angelika Peer and Martin Buss. 2008. A New Admittance-Type Haptic Interface for Bimanual Manipulations. *IEEE/ASME Transactions on Mechatronics* 13, 4 (2008), 416–428. DOI: http://dx.doi.org/10.1109/TMECH.2008.2001690

35. Christian Reeks, Marc G. Carmichael, Dikai Liu, and Kenneth J. Waldron. 2016. Angled Sensor Configuration Capable of Measuring Tri-Axial Forces for pHRI. In *Proceedings of the 2016 IEEE International Conference on Robotics and Automation (ICRA)*. 3089–3094. DOI: http://dx.doi.org/10.1109/ICRA.2016.7487475

36. Eckard Riedenklau. 2016. *Development of Actuated Tangible User Interfaces: New Interaction Concepts and Evaluation Methods*. Ph.D. Dissertation. http://pub.uni-bielefeld.de/publication/2900748

37. Dan Rosenfeld, Michael Zawadzki, Jeremi Sudol, and Ken Perlin. 2004. Physical Objects as Bidirectional User Interface Elements. *IEEE Computer Graphics and Applications* 24, 1 (2004), 44–49. DOI: http://dx.doi.org/10.1109/MCG.2004.1255808

38. Michael Rubenstein, Christian Ahler, and Radhika Nagpal. 2012. Kilobot: A Low Cost Scalable Robot System for Collective Behaviors. In *Proceedings of the 2012 IEEE International Conference on Robotics and Automation (ICRA)*. 3293–3298. DOI: http://dx.doi.org/10.1109/ICRA.2012.6224638

39. Mine Sarac, Mehmet Alper Ergin, Ahmetcan Erdogan, and Volkan Patoglu. 2014. ASSISTON-MOBILE: A Series Elastic Holonomic Mobile Platform for Upper Extremity Rehabilitation. *Robotica* 32, 08 (2014), 1433–1459. DOI: http://dx.doi.org/10.1017/S0263574714002367

40. Masanori Sugimoto, Tomoki Fujita, Haipeng Mi, and Aleksander Krzywinski. 2011. RoboTable2: A Novel Programming Environment using Physical Robots on a Tabletop Platform. In *Proceedings of the 8th International Conference on Advances in Computer Entertainment Technology*. 10:1–10:8. DOI: http://dx.doi.org/10.1145/2071423.2071436

41. Dimitar Valkov, Andreas Mantler, and Klaus Hinrichs. 2013. Haptic Props: Semi-actuated Tangible Props for Haptic Interaction on the Surface. In *Proceedings of the Adjunct Publication of the 26th Annual ACM Symposium on User Interface Software and Technology*. 113–114. DOI:http://dx.doi.org/10.1145/2508468.2514736

42. Malte Weiss, Florian Schwarz, Simon Jakubowski, and Jan Borchers. 2010. Madgets: Actuating Widgets on Interactive Tabletops. In *Proceedings of the 23rd Annual ACM Symposium on User Interface Software and Technology*. 293–302. DOI: http://dx.doi.org/10.1145/1866029.1866075